Effect of acceleration threshold on the phase transition in a cellular automaton traffic flow model*

Jin Cheng-Jie(金诚杰)[a)†], Wang Wei(王 炜)[a)], Gao Kun(高 坤)[b)], and Jiang Rui(姜 锐)[c)]

[a)] *School of Transportation, Southeast University of China, Nanjing* 210096, *China*

[b)] *Physics and Biology Unit, Okinawa Institute of Science and Technology, Okinawa* 904-0411, *Japan*

[c)] *School of Engineering Science, University of Science and Technology of China, Hefei* 230026, *China*

(Received 11 November 2010; revised manuscript received 15 December 2010)

In this paper, we incorporate new parameters into a cellular automaton traffic flow model proposed in our previous paper [Jin *et al.* 2010 *J. Stat. Mech.* **2010** P03018]. Through these parameters, we adjust the anticipated velocity and the acceleration threshold separately. It turns out that the flow rate of synchronized flow mainly changes with the anticipated velocity, and the $F \to S$ phase transition feature mainly changes with the acceleration threshold. Therefore, we conclude that the acceleration threshold is the major factor affecting the $F \to S$ phase transition.

Keywords: traffic flow, cellular automaton, synchronized flow, phase transition

PACS: 45.70.Vn, 05.40.–a, 02.60.Cb **DOI:** 10.1088/1674-1056/20/6/064501

1. Introduction

Traffic flow is an interdisciplinary research area over engineering, physics, mathematics and so on. Among the approaches and theories used in this area, statistical physics shows special advantages and has greatly impelled the research of traffic dynamics and traffic systems.[1−12] Phase transitions were introduced into a traffic flow system in order to explain the emergence of congested traffic. Before the concept of synchronized flow was proposed, traffic states were simply divided into two phases, the free flow phase (F) and the congested flow phase.

Based on the empirical data, Kerner realized that the two-phase division is too rough to describe so many details of traffic flow. Thus, congested flow is further classified into synchronized flow (S) and jam (J). The transitions among the three phases are of the first order. Usually, before jams come to form, traffic flow turns from free flow to synchronized flow and after that jams spontaneously emerge somewhere inside the synchronized flow region. The theory is called the three-phase traffic theory.[12]

So far, there have been some models developed in the framework of three-phase traffic theory, for example, the KKW models,[13,14] Lee model,[15] the MCD models,[16,17] and the VDE models.[18,19] In a recent paper,[20] the authors have proposed a new cellular automaton (CA) model, which focuses on the $S \to J$ transition. It has been shown that slow-to-start effect might not be the only possible mechanism responsible for first-order $S \to J$ transition.

This paper studies $F \to S$ transition by using the CA model. We have incorporated some new parameters into the model. Through these parameters, we adjust the anticipated velocity and the acceleration threshold separately. It is found that the flow rate of synchronized flow mainly changes with the anticipated velocity and the $F \to S$ phase transition feature mainly changes with the acceleration threshold.

The paper is organized as follows. In Section 2, we review our model. In Section 3, we present and discuss the simulation results. The conclusion is given in Section 4.

2. Model rules

For self-consistency, we describe the model in this section. Motivated by the idea of "deceleration limitation" in Refs. [15] and [21], we designed the velocity-updating rule with anticipated deceleration (AD) $a_{\rm AD}$ in the model, with which drivers prefer to decelerate when necessary. Different values of $a_{\rm AD}$ could reflect different characteristics and different driving strategies of the drivers. The rules of the model are designed to guarantee safety if the drivers really decelerate with

*Project supported by the National Natural Science Foundation of China (Grant Nos. 10872194 and 50738001).

†Corresponding author. E-mail: yitaikongtiao@gmail.com

© 2011 Chinese Physical Society and IOP Publishing Ltd

$a_{\rm AD}$. The anticipated safe velocity $V_{\rm anti}$ ($a_{\rm AD}$, $d_{\rm gap}$) is the maximum of v satisfying the inequality

$$B(v, a_{\rm AD}) \leq d_{\rm gap}. \tag{1}$$

Here $B(v, a_{\rm AD})$ is the whole distance that a vehicle travels before stopping if it keeps decelerating with $a_{\rm AD}$ from an initial velocity v. In cellular automaton models, function $B(v, a_{\rm AD})$ is often discretized. Suppose $m = {\rm int}(v/|a_{\rm AD}|)$, then $B(v, a_{\rm AD})$ can be calculated as

$$\begin{aligned} B(v, a_{\rm AD}) &= v + (v + a_{\rm AD}) + (v + 2a_{\rm AD}) + \cdots \\ &\quad + (v + ma_{\rm AD}) \\ &= (2v + ma_{\rm AD})(m + 1)/2. \end{aligned} \tag{2}$$

With the anticipated safe velocity $V_{\rm anti}(a_{\rm AD}, d_{\rm gap})$ calculated above, the model rules are executed on all vehicles in parallel as follows:

(i) Determining the randomization probability (slow-to-start rule[22])

$$p_n(v) = \begin{cases} p_0, & \text{when } v_n > 0, \\ p_d, & \text{when } v_n = 0. \end{cases}$$

(ii) Estimating the virtual velocity of the front vehicle (vehicle $n-1$)[23]

$$v'_{n-1} \to \min\{v_{\max} - 1, \max\{0, V_{\rm anti}(a_{\rm AD}, (d_{\rm gap})_{n-1}) - 1\}, v_{n-1}\}.$$

(iii) Deterministic acceleration or deceleration

$$v_n \to \begin{cases} \min\{v_n + 1, v_{\max}\}, & \text{when } v_n < (d_{\rm gap})_n + v'_{n-1} \quad \text{(acceleration)}, \\ V_{\rm anti}(a_{\rm AD}, (d_{\rm gap})_n + v'_{n-1}), & \text{when } v_n \geq (d_{\rm gap})_n + v'_{n-1} \quad \text{(deceleration)}. \end{cases} \tag{3}$$

(iv) Randomization

$v_n \to \max\{v_n - 1, 0\}$, with probability p_n.

(v) Updating positions

$$x_n(t+1) \to x_n + v_n.$$

In the above formulations, $x_n(t)$ and $v_n(t)$ are the position and velocity of vehicle n at time t; vehicle $n-1$ precedes vehicle n; $(d_{\rm gap})_n$ is the distance between vehicle n and vehicle $n-1$; and $v_{\max}$ is the speed-limitation of the vehicles.

Inequality (1) has guaranteed a vehicle moving with the velocity $V_{\rm anti}(a_{\rm AD}, d_{\rm gap})$ can brake till stop before it hits the front vehicle. If satisfied, then driving with velocity no larger than $V_{\rm anti}(a_{\rm AD}, d_{\rm gap})$ and braking with AD would always be safe. On the other hand, it should be noted that $a_{\rm AD}$ is only an anticipated deceleration rather than a deceleration limitation as in Refs. [15] and [21]. If the deceleration has to be larger than $|a_{\rm AD}|$ (especially in emergencies), it will be allowed in our model. Therefore vehicle collisions can be totally avoided. This is different from Lee model,[15] in which deceleration never exceeds the limitation so that collisions sometimes might happen.

In Eq. (3), one can see that whether a vehicle accelerates or not depends on the relationship between v_n and $(d_{\rm gap})_n + v'_{n-1}$. Such a kind of relationship is called "acceleration threshold" in this paper.

We would like to mention that although the model rules presented here look different from that in Ref. [20], they are actually the same because $V_{\rm anti}(a_{\rm AD}, d_{\rm gap}) = v_n + A(d_{\rm gap}, v_n, a_{\rm AD})$. Here $A(d_{\rm gap}, v_n, a_{\rm AD})$ is the deceleration function defined in Ref. [20]. We believe the model rule in this paper is more straightforward to understand.

3. Simulated results

In this section we present the simulated results of our model and mainly focus on the $F \to S$ phase transition features. Our simulations are carried out on a homogeneous circular road of length $L = 8000$ cells; each cell is set to be 1 m long and each time step corresponds to 1 s. Each vehicle occupies 8 cells; the maximum velocity is set to 32 m/s and the randomization parameters are set to $p_0 = 0.1$ and $p_d = 0.4$.

In Fig. 1, we show the fundamental diagrams of the model under different values of $a_{\rm AD}$. We obtain the fundamental diagrams from two different types of initial states: the homogeneous state and the completely jamming state.[22] In Fig. 1(a), we set $a_{\rm AD} = -4$ m/s^2, which is close to the comfortable deceleration under normal situations (which is -3 m/s^2 in Ref. [15]). The fundamental diagram has three branches, corresponding to the three traffic phases re-

spectively. Branch AE corresponds to free flow, in which the low-density branch AB is stable but the relatively high-density branch BE is metastable. First-order $F \to S$ phase transition may happen from these metastable states (see Fig. 2(a)). Branch BD corresponds to synchronized flow. Likewise, when the density is low, branch BC is stable, corresponding to a mixture of free flow and synchronized flow (see Fig. 2(b)). On the other hand, when the density is high, branch CD is metastable; first-order phase transition to jams may happen (see Fig. 2(c)). Finally, branch CF corresponds to wide-moving jams and it is always stable.

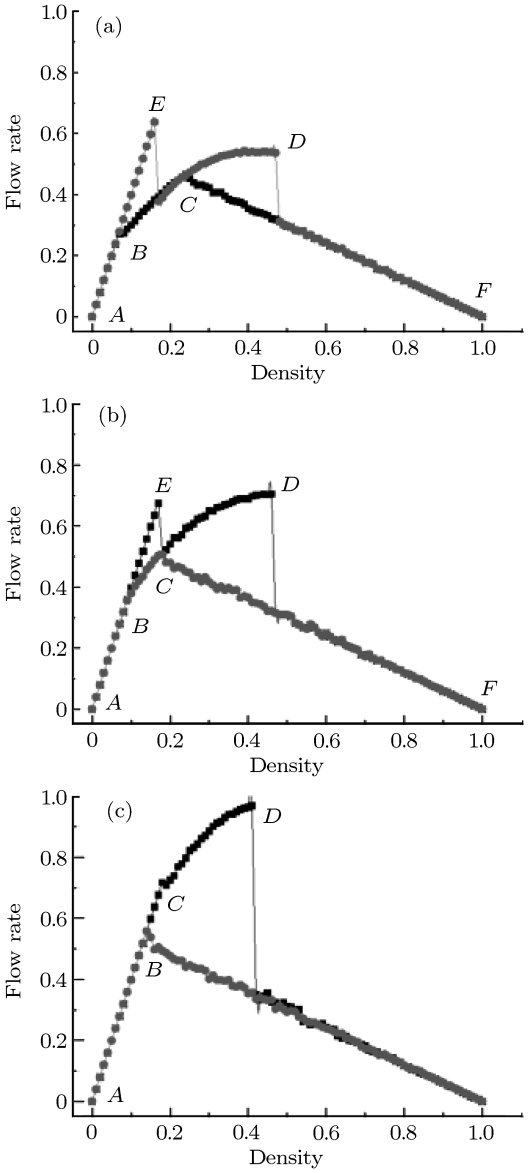


Fig. 1. Fundamental diagrams of the model: (a) $a_{\rm AD} = -4$ m/s^2. (b) $a_{\rm AD} = -8$ m/s^2. (c) $a_{\rm AD} = -16$ m/s^2.

With the increase of $|a_{\rm AD}|$, one can see that the first order $F \to S$ phase transition gradually disappears (c.f. Figs. 1(b) and 1(c)). Therefore, a naive explanation is that $a_{\rm AD}$ is responsible for the type of $F \to S$ phase transition. Nevertheless, a closer look at the fundamental diagram shown in Fig. 1 indicates that with the increase of $|a_{\rm AD}|$, the free flow branch does not shrink. Instead, it slightly expands. At the same time, the synchronized flow branch gradually enhances. When $a_{\rm AD} = -16$ m/s^2, the synchronized flow branch completely covers the free flow branch, so that the first-order phase transition disappears.

As one can see in Eq. (3), $a_{\rm AD}$ appears in both sides of the acceleration threshold (note that v'_{n-1} is a function of $a_{\rm AD}$: $v'_{n-1} = v'_{n-1}(a_{\rm AD})$). In order to find out the exact reason why free flow branch expands and synchronized flow branch enhances, we introduce $a_{\rm AD1}$ and $a_{\rm AD2}$ and modify Eq. (3) as

$$v_n \to \begin{cases} \min\{v_n + 1, v_{\max}\}, \\ \text{when } v_n < (d_{\rm gap})_n + v'_{n-1}(a_{\rm AD2}); \\ V_{\rm anti}(a_{\rm AD1}, (d_{\rm gap})_n + v'_{n-1}(a_{\rm AD1})), \\ \text{when } v_n \geq (d_{\rm gap})_n + v'_{n-1}(a_{\rm AD2}). \end{cases} \tag{4}$$

In Fig. 3(a), we fix $a_{\rm AD1} = -4$ m/s^2 and change only $a_{\rm AD2}$. With the increase of $|a_{\rm AD2}|$, the right-hand side of acceleration threshold increases and the free flow branch gradually expands. The synchronized flow branch essentially does not change. We fix $a_{\rm AD2} = -4$ m/s^2 and change only $a_{\rm AD1}$ in Fig. 3(b). With the increase of $|a_{\rm AD1}|$, the free flow branch essentially does not change and the synchronized flow branch enhances.

Based on the results, we argue that changing the acceleration threshold mainly affects maximum free flow rate (i.e., the critical density of $F \to S$ phase transition): the free flow branch expands with the increase (decrease) of the right (left) hand side of the acceleration threshold and *vice versa*. On the other hand, changing the anticipated velocity $V_{\rm anti}$ mainly affects the synchronized flow rate.[1)] To further verify the argument, we introduce another 3 parameters: α, β_1 and β_2, and further modify Eq. (3) as

[1)] Note that the change of acceleration threshold and $V_{\rm anti}$ needs to be restricted within a certain range. Otherwise the argument is invalid. For instance, if $V_{\rm anti}$ is changed to $V_{\rm anti} = \min(v_n + 1, v_{\max})$, then the model becomes qualitatively different. Moreover, also note that sometimes acceleration threshold might also affect synchronized flow rate, (see e.g., Fig. 6).

$$v_n \to \begin{cases} \min\{v_n + 1, v_{\max}\}, & \text{when } (1-\alpha)v_n + \alpha B(v_n, a_{\rm AD}) < (d_{\rm gap})_n + \beta_2 v'_{n-1}; \\ V_{\rm anti}(a_{\rm AD}, (d_{\rm gap})_n + \beta_1 v'_{n-1}), & \text{when } (1-\alpha)v_n + \alpha B(v_n, a_{\rm AD}) \geq (d_{\rm gap})_n + \beta_2 v'_{n-1}. \end{cases} \tag{5}$$

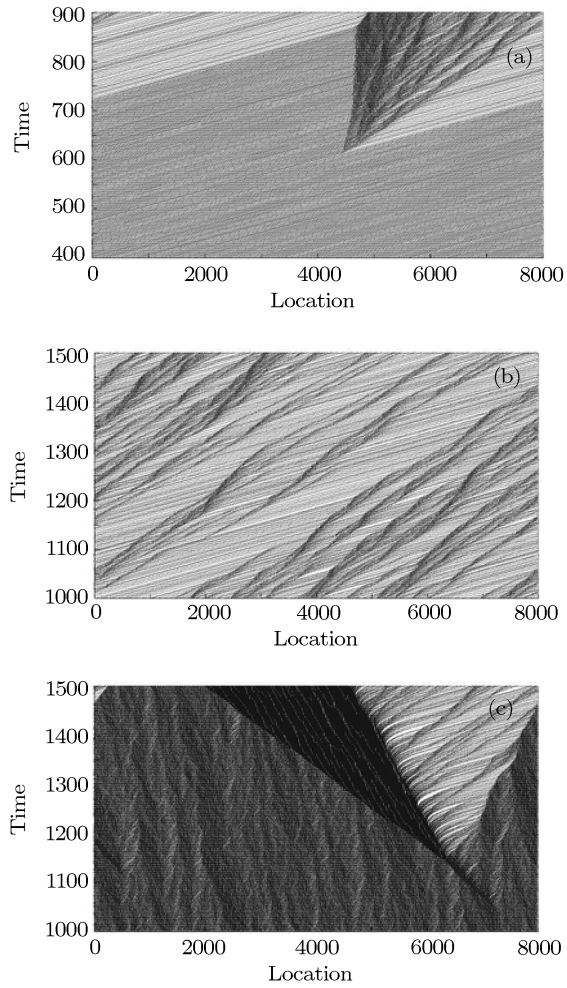


Fig. 2. Typical spatiotemporal diagrams when $a_{\rm AD} = -8$ m/s^2: (a) $F \to S$, $\rho = 0.18$, (b) $\rho = 0.15$, (c) $S \to J$, $\rho = 0.5$.

Note that since $B(v_n, a_{\rm AD}) \geq v_n$, the left-hand side of acceleration threshold increases with the increase of α. Therefore, we expect that the free flow branch shrinks with the increase of α. As can be seen in Fig. 4, the simulated result is consistent with our expectation.

In Fig. 5, β_1 changes and other parameters are fixed. In Fig. 6, β_2 changes and other parameters are fixed. With the decrease of β_1, the flow rate of synchronized flow drops remarkably but the critical density of $F \to S$ phase transition remains unchanged. On the other hand, the decrease of β_2 leads to slightly higher flow rate of synchronized flow, but it makes the critical density much smaller.

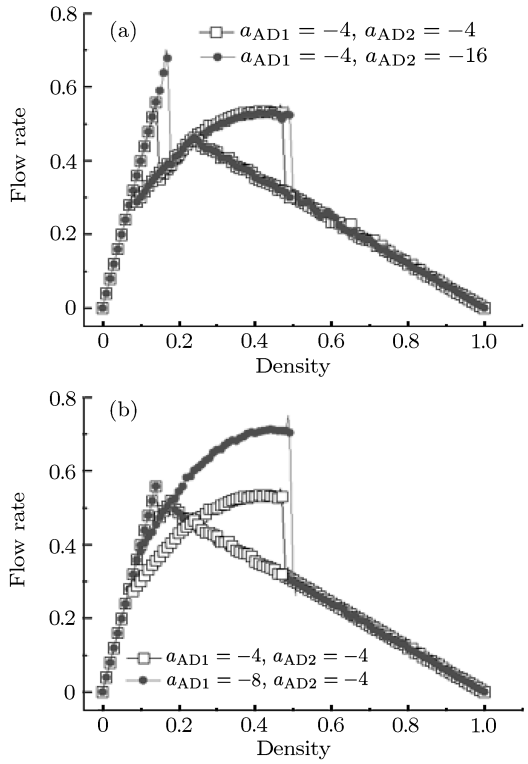


Fig. 3. Fundamental diagrams of our model under different values of $a_{\rm AD}$. (a) $a_{\rm AD1} = -4$ m/s^2, (b) $a_{\rm AD2} = -4$ m/s^2.

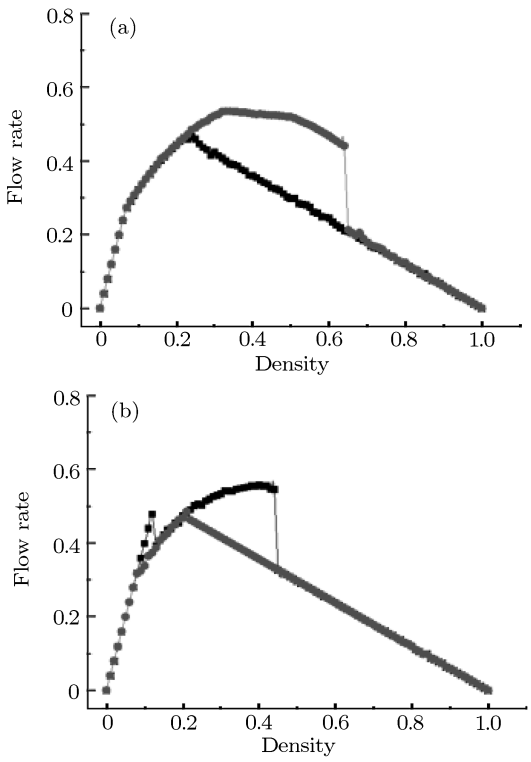


Fig. 4. Fundamental diagrams of our model when $a_{\rm AD} = -4$ m/s^2: (a) $\alpha = 1$, (b) $\alpha = 0.25$.

Consequently, we conclude that $F \rightarrow S$ phase transition mainly depends on the acceleration threshold. When the right- (left-) hand side of the acceleration threshold decreases (increases), which implies that drivers become more careful and cautious, the first-order phase transition might disappear.

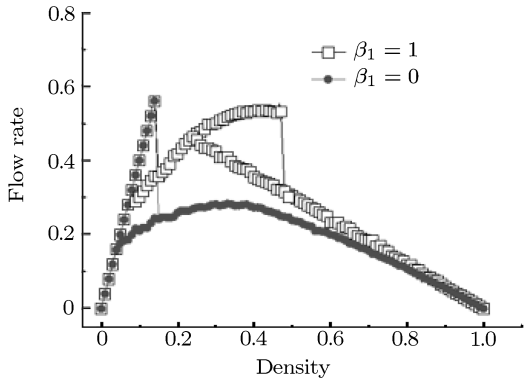


Fig. 5. Fundamental diagrams of our model when $a_{\rm AD} = -4$ m/s^2, $\alpha = 0$, $\beta_2 = 1$.

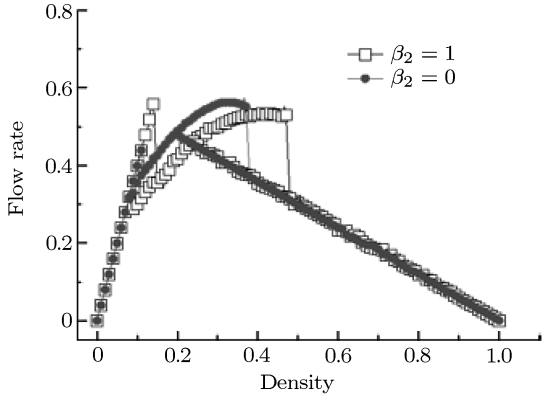


Fig. 6. Fundamental diagrams of our model when $a_{\rm AD} = -4$ m/s^2, $\alpha = 0$, $\beta_1 = 1$.

We also would like to discuss the situation of $F \rightarrow S$ phase transition in several other models. We argue that the main differences between the FMCD[17] and the MCD models,[16] and between the MVDE[19] and the VDE models[18] also lie in the acceleration threshold. By changing the acceleration threshold, the FMCD and the MVDE models could successfully reproduce the first-order $F \rightarrow S$ phase transition, while the MCD and VDE models could not. Similarly, in Lee model,[15] if we change the acceleration threshold by fixing the optimistic parameter $\gamma = 1$, the first-order $F \rightarrow S$ phase transition also disappears.

Finally we would like to point out that although the acceleration threshold does not (or only slightly) essentially affect the flow rate of synchronized flow, it changes the property of synchronized flow. For instance, figure 7 shows the velocity snapshots of synchronized flow at different values of α. One can see that with the increase of α, the synchronized flow becomes more and more homogeneous.

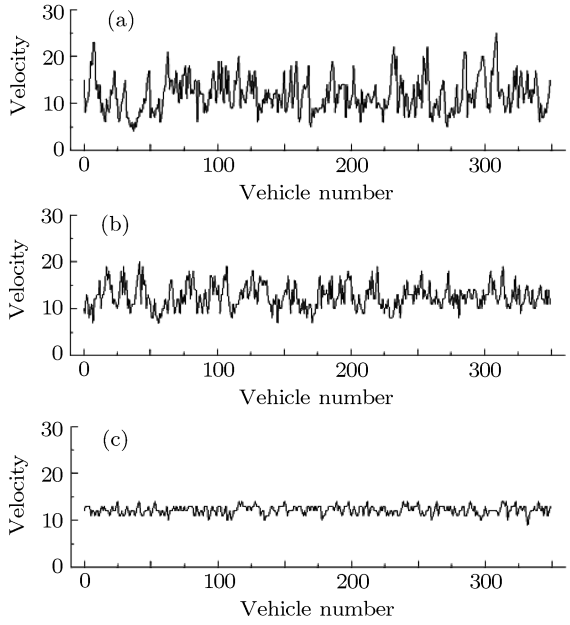


Fig. 7. Velocity snapshots for the traffic flow when $a_{\rm AD} = -4$ m/s^2 and $\rho = 0.35$. (a) $\alpha = 0$; (b) $\alpha = 0.25$; (c) $\alpha = 1$.

4. Conclusion

In this paper, we have studied a cellular automaton model proposed in our previous paper[20] in more details. We introduce some new parameters into the model and change them separately. Through the investigations, it is found that the anticipated velocity $V_{\rm anti}$ mainly affects the synchronized flow rate and the $F \rightarrow S$ phase transition feature does not essentially change with it. On the other hand, the acceleration threshold mainly influences the $F \rightarrow S$ phase transition features. With the increase (decrease) of the left- (right-) hand side of the acceleration threshold, the free flow branch shrinks and the $F \rightarrow S$ phase transition gradually turns from first-order to continuous. At the same time, the fluctuations inside the synchronized flow weakens, it becomes more homogeneous. Therefore, we conclude that the $F \rightarrow S$ phase transition is mainly affected by the acceleration threshold.

Acknowledgements

The authors are grateful to an anonymous referee for their valuable comments.

References

[1] Helbing D 2001 *Rev. Mod. Phys.* **73** 1067

[2] Chowdhury D, Santen L and Schadschneider A 2000 *Phys. Rep.* **329** 199

[3] Mahnke R, Kaupužs J and Lubashevsky I 2005 *Phys. Rep.* **408** 1

[4] Maerivoet S and De Moor B 2005 *Phys. Rep.* **419** 1

[5] Nagatani T 2002 *Rep. Prog. Phys.* **65** 1331

[6] Xue Y 2002 *Chin. Phys.* **11** 1128

[7] Li K P and Gao Z Y 2005 *Chin. Phys.* **14** 930

[8] Li L and Shi P F 2005 *Chin. Phys.* **14** 576

[9] Tang C F, Jiang R and Wu Q S 2007 *Chin. Phys.* **16** 1570

[10] Gao K, Wang B H, Fu C J and Lu Y F 2007 *Chin. Phys.* **16** 3483

[11] Jiang R, Jin W L and Wu Q S 2008 *Chin. Phys.* B **17** 829

[12] Kerner B S 2004 *The Physics of Traffic* (Berlin: Springer)

[13] Kerner B S, Klenov S L and Wolf D E 2002 *J. Phys.* A: *Math. Gen.* **35** 9971

[14] Kerner B S and Klenov S L 2002 *J. Phys.* A: *Math. Gen.* **35** L31

[15] Lee H K, Barlovic R, Schreckenberg M and Kim D 2004 *Phys. Rev. Lett.* **92** 23870

[16] Jiang R and Wu Q S 2003 *J. Phys.* A: *Math. Gen.* **36** 381

[17] Jiang R and Wu Q S 2005 *Eur. Phys. J.* B **46** 581

[18] Gao K, Jiang R, Hu S X, Wang B H and Wu Q S 2007 *Phys. Rev.* E **76** 026105

[19] Gao K, Jiang R, Wang B H and Wu Q S 2009 *Physica* A **388** 3233

[20] Jin C J, Wang W, Jiang R and Gao K 2010 *J. Stat. Mech.* **2010** P03018

[21] Krauss S, Wagner P and Gawron C 1997 *Phys. Rev.* E **55** 5597

[22] Barlovic R, Santen L, Schadschneider A and Schreckenberg M 1998 *Eur. Phys. J.* B **5** 793

[23] Li X B, Wu Q S and Jiang R 2001 *Phys. Rev.* E **64** 066l28